

High Temperature Deformation Behavior of TC17 Alloy

Chen Wang

School of Materials Engineering, Xi'an Aeronautical University, Xi'an, China

Email: chenwang@163.com

How to cite this paper: Wang, C. (2018) High Temperature Deformation Behavior of TC17 Alloy. *Materials Sciences and Applications*, 9, 732-739.
<https://doi.org/10.4236/msa.2018.99053>

Received: July 19, 2018

Accepted: August 10, 2018

Published: August 13, 2018

Copyright © 2018 by author and Scientific Research Publishing Inc.

This work is licensed under the Creative Commons Attribution International License (CC BY 4.0).

<http://creativecommons.org/licenses/by/4.0/>



Open Access

Abstract

The high temperature deformation behavior and microstructures evolution of TC17 alloy in the temperature range of 820°C - 930°C, strain rate range of 0.01 s⁻¹ - 10 s⁻¹ and height direction reduction of 20% - 80% have been studied by hot compressing testing. The microstructures of TC17 alloy were observed and analyzed using Olympus/PMG3 optical microscope. The flow stresses were correlated with strain rate and the temperature by the constitutive equation. The results show that the flow stress of TC17 alloy increase quickly with the strain, then decrease with a steady value. The deformation activation energy obtained in the $\alpha + \beta$ region for TC17 was 407 kJ/mol, and in the β region was 155 kJ/mol. It was also found that the degree of dynamic globularization of α phase increases with increasing strains, increasing temperature and decreasing strain rate in $\alpha + \beta$ region, the dynamic re-crystallization is obvious at low strain rate and dynamic recovery is obvious at high strain rate in β region.

Keywords

TC17 Alloy, High Temperature Deformation, Flow Stress Model, Microstructure, Dynamic Recovery

1. Introduction

The nominal composition of TC17 titanium alloy is Ti-5Al-2Sn-2Zr-4Mo-4Cr, and its using temperature reaches 427°C. The conventional forging process is two-phase regions forging for equiaxed structure at a temperature range from 816°C to 857°C and β forging for the basket structure at a temperature range from 899°C to 977°C [1].

The research of high temperature deformation behavior of materials is mainly to analyze the microstructure evolution and microscopic deformation mechan-

ism of materials by changing the influencing factors such as deformation amount, deformation temperature and deformation rate. There are many works conducted in this field [2] [3] [4] [5]. S.L. Semiatin [6] and his team used Ti-1100 titanium alloy as the research object, calculating and analyzing the deformation activation energy and deformation mechanism of this alloy undergoing thermal deformation in the β single-phase region and the $\alpha + \beta$ two-phase region; Zhao Yongqing [7] [8] [9] and his team studied the effects of thermal deformation parameters on the high temperature rheological behavior, microstructure and microstructure evolution of titanium alloys. Three different microstructures of TC4-DT titanium alloy thermal simulation compression experiments were conducted to investigate the relationship between flow stress and microstructure by Hong Quan [10] and his team.

In this paper, the true stress-true strain relationship curve of TC17 is studied, the activation energy of the alloy in the two-phase region and the β -phase phase is obtained, and the microstructure evolution under different deformation conditions is analyzed.

2. Experiment

The experimental material was supplied in form of forged bar with diameter of 46 mm. Its chemical composition in wt. % was: 5.09 Al, 2.16 Sn, 2.00 Zr, 4.32 Mo, 3.94 Cr, 0.013 N, 0.09 O, 0.003 H, and Ti (balance). The nominal beta transus temperature for this alloy is $885^{\circ}\text{C} \pm 5^{\circ}\text{C}$. The initial microstructure of TC17 alloy after β -phase forging is shown in **Figure 1**, which is the basket organization.

Hot compressive deformation behavior of TC17 alloy at elevated temperatures was characterized by isothermal compression tests on Gleeble 1500. Cylindrical specimens of 8 mm diameter and 12mm length were machined from the bar. The compressive tests were performed in deformation temperature ranging of $820^{\circ}\text{C} - 930^{\circ}\text{C}$ and at strain rates from 0.01 s^{-1} to 10 s^{-1} . The specimens were heated to the compression temperature at 5°C/s , held at least 300 s and then deformed up to 20% - 80% height reduction under constant strain rate. After the test, the sample was water quenched to retain its high temperature structure. The microstructure of TC17 alloy was observed and analyzed using Olympus/PMG3 optical microscope.

3. Results and Discussion

3.1. Flow Behavior

Figure 2 shows the true stress—true strain (σ - $\dot{\epsilon}$) curve of TC17 alloy which is under phase transformation (820°C , 850°C), near the phase transition point (880°C and 890°C) and above the transformation point (900°C and 930°C) with deformation of 60%.

It can be seen from **Figure 2** that under different deformation conditions, the true stress-true strain curve of TC17 alloy has almost the same trend, that is the stress value increases rapidly in the initial stage of deformation and after reaching

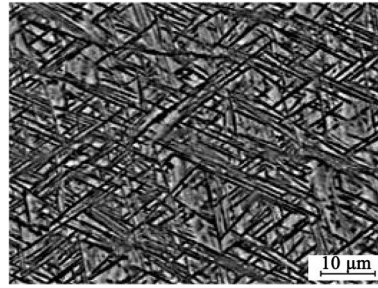


Figure 1. Initial microstructure of TC17 alloy.

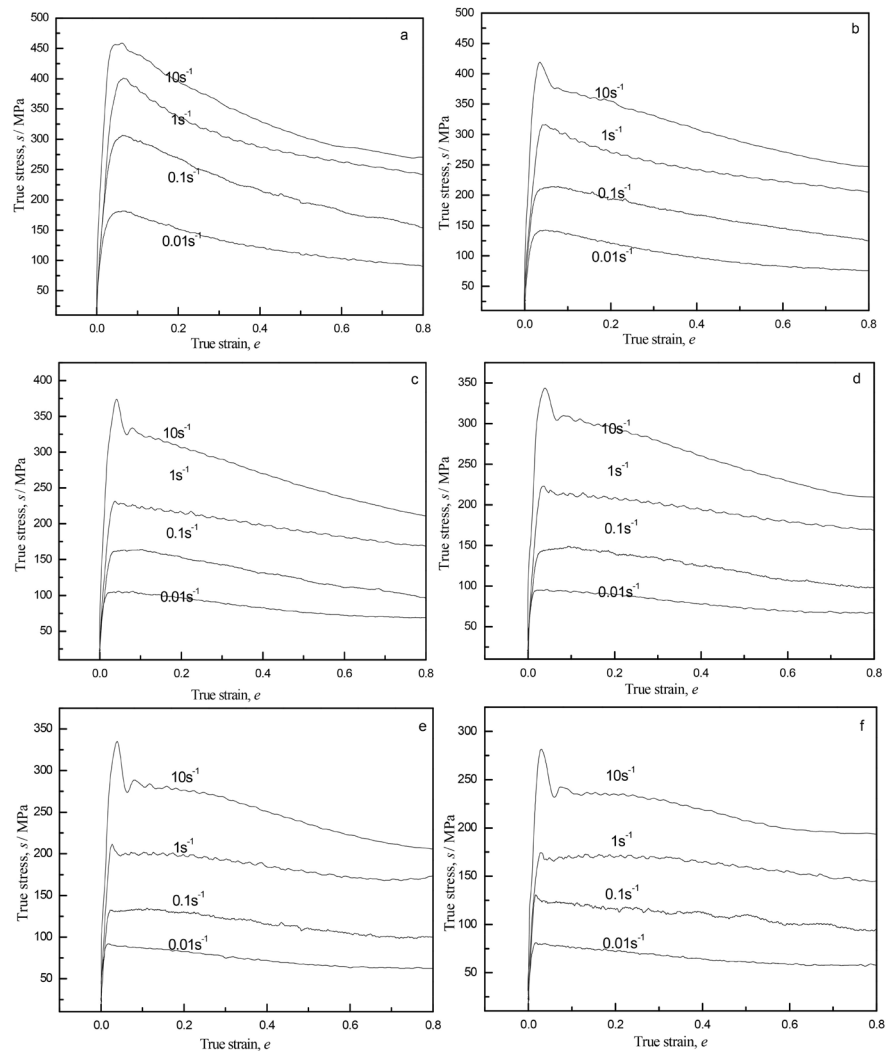


Figure 2. Flow stress curves of TC17 titanium alloy compressed at different deformation conditions. (a) 820°C; (b) 850°C; (c) 880°C; (d) 890°C; (e) 900°C; (f) 930°C.

the maximum value, the stress value decreases. After the strain reaches a certain value, it basically stabilizes. The reason is that both hardening and softening mechanism of the alloy work during the hot deformation process. In the initial stage of deformation, the dislocation density increases to a large extent, and the dislocation motion is insufficient to compensate for the work hardening, result-

ing in a rapid increase in the stress value; As the compression test progresses, dynamic recovery and dynamic re-crystallization behavior occur inside the alloy, resulting flow softening and work hardening reach a dynamic equilibrium, a gentle stress curve appear [11] [12].

It can be seen from **Figure 2(e)** and **Figure 2(f)** that stress oscillation occurs when the deformation temperature is close to or above the phase transition point, and strain rate at 10 s^{-1} . That is because the dislocation pinning mechanism or movable dislocation increases in grain boundaries [13]. It can also be seen from the curve that when it is below the phase transition point ($820^\circ\text{C} - 880^\circ\text{C}$), the alloy exhibits a dynamic re-crystallization curve characteristics during thermal deformation, and when it is above the phase transition point, it shows dynamic recovery.

In summary, the flow stress behavior of TC17 alloy is sensitive to all three deformation parameters. The softening mechanism cannot be determined by merely observing the characteristics of the rheological curve, which will be further described with the microstructure of the alloy under different deformation conditions in the following paper.

3.2. Constitutive Relationship and Activation Energy

The flow stress of a material is generally represented by three forms of equations [14] [15]. In this paper, the Arrhenius relationship is selected as the formula to describe the behavior of heat-activated steady-state deformation is modifying, and to describe the constitutive relationship of TC17 alloy.

$$\dot{\epsilon} = A [\sinh(\alpha\sigma)]^n \exp(-Q/RT) \quad (1)$$

A , α and n are constants independent of the deformation temperature.

It is assumed that the deformation temperature does not affect the deformation activation energy, taking natural logarithm in it and we get this,

$$\ln \dot{\epsilon} = \ln A_3 + (-Q/RT) + n \ln [\sinh(\alpha\sigma)] \quad (2)$$

Substituting the steady flow stress of TC17 alloy with strain rate under different deformation conditions into Equation (2), using $\ln [\sinh(\alpha\sigma)]$ with $\ln \dot{\epsilon}$, $\ln [\sinh(\alpha\sigma)]$ with $1000/T$ to make diagram, and using origin for linear regression, relationship between steady flow stress and deformation rate and deformation temperature shown in **Figure 3**.

It can be seen from **Figure 3** that the steady flow stress is related to the strain rate when the TC17 alloy is deformed at different temperatures. When deforming occur below the phase transition point ($820^\circ\text{C} - 880^\circ\text{C}$), the slope of the curve changes greatly, indicating that the strain rate has a greater influence on the flow stress, and the alloy is sensitive to strain rate; when deforming occur above the phase transition point, the slopes of the curves are nearly equal. It can be seen from **Figure 2** that the deformation temperature has a significant influence on the flow stress, and the flow stress decreases as the deformation temperature increases. From **Figure 3**, the reciprocal of the strain rate sensitivity coeffi-

cient n_1 and the value of the constant β can be obtained. Since α , β and n_1 is satisfied $\alpha = \beta/n_1$, the α value is determined to be 0.0089. After deforming (2), and computing partial derivation

$$Q = R \times \frac{\partial \ln \dot{\epsilon}}{\partial \ln(\sinh(a\sigma))} \times \frac{\partial \ln(\sinh(a\sigma))}{\partial \ln(1/T)} \quad (3)$$

$\frac{\partial \ln \dot{\epsilon}}{\partial \ln(\sinh(a\sigma))}$ and $\frac{\partial \ln(\sinh(a\sigma))}{\partial \ln(1/T)}$ are the slopes of the curves in **Figure 3(a)** and **Figure 3(b)**.

The deformation activation energy obtained in the $\alpha + \beta$ region for TC17 was 407 kJ/mol, and in the β region was 155 kJ/mol.

3.3. Microstructural Observations

Figure 4 shows the microstructures of the specimens at different deformation conditions.

It can be seen from **Figure 4** that when 20% of the alloy deforms, the α phase does not change substantially; as the compression amount increases, the α phase parallel to the compression direction is first spheroidized, the length of the α phase is significantly shortened, and the proportion of spheroidized α phase is significantly increased; When the amount of compression is 80%, the α phase is all globalized. This is mainly due to the increase of defects in the α phase when the amount of deformation is large, which is favorable for α spheroidization behavior (**Figure 4(d)**).

Figure 5 shows the microstructures of the specimens at different deformation conditions (850°C, 0.1 s⁻¹ and 10 s⁻¹, with a compression of 60%). It can be seen from **Figure 5** that when the strain rate is 0.1 s⁻¹, the spheroidization of the α phase is more obvious due to the sufficient spheroidization time. As the strain rate increases, the dislocation density increases during the deforming, the softening mechanism is too late to occur, and the rheological instability appears. That is the wavy and stress discontinuous yielding phenomenon reflected in **Figure 2**.

It can be known from **Figure 6(a)** and **Figure 6(b)** that when the alloy is deformed below the transformation point, the degree of spheroidization increases as the temperature increases. When deformation occurs above the phase transition point, if it is at low strain rates, the grains are elongated along the metal flow direction, and a small amount of equiaxed recrystallized grains appear (**Figure 6(c)**); and if it is at high strain rates, a curved deformation zone appears in the structure (**Figure 6(d)**). At this time, there is no obvious recrystallized grain in the alloy, and the dynamic recovery behavior is dominant.

4. Conclusions

TC17 alloy has been studied during hot deformation both in the $\alpha + \beta$ region and

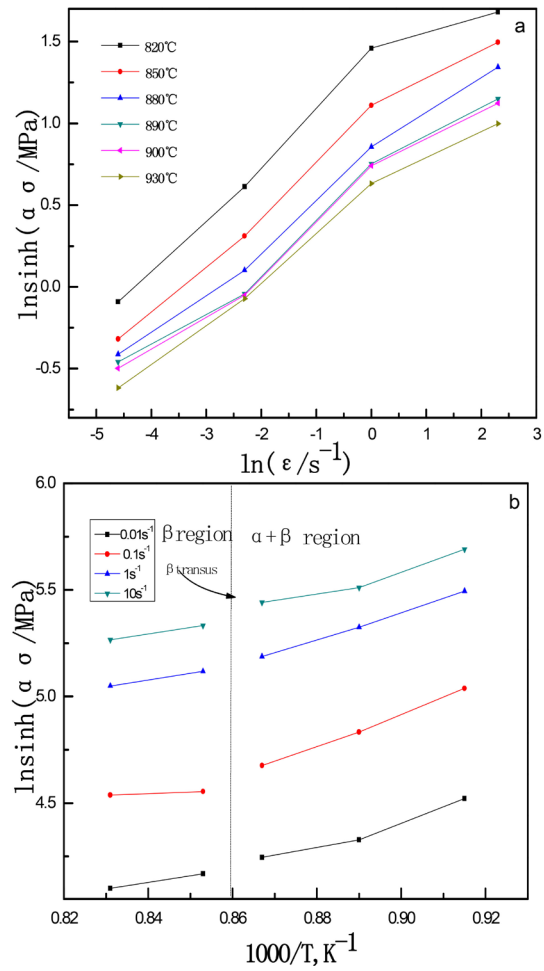


Figure 3. (a) The relationship between flow stress and strain rate of TC17 alloy; (b) The relationship between flow stress and temperature of TC17 alloy.

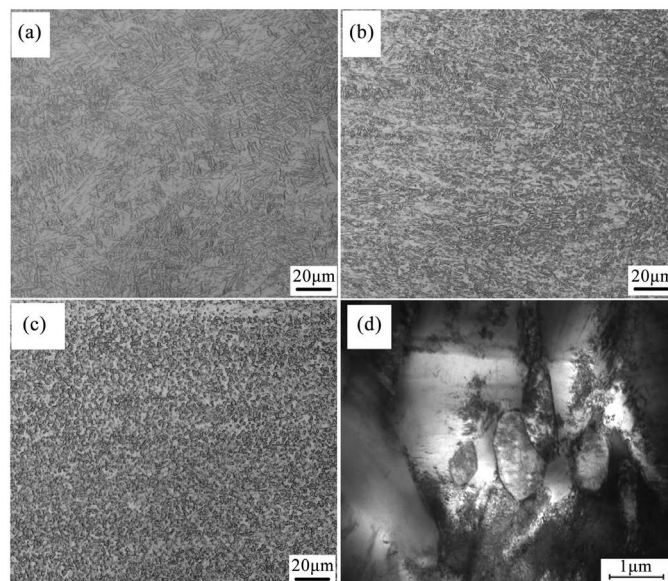


Figure 4. Microstructures of TC17 alloy deformed at: (a) 820°C 0.01 s⁻¹ 20%; (b) 820°C 0.01 s⁻¹ 40%; (c) 820°C 0.01 s⁻¹ 80%; (d) 820°C 0.01 s⁻¹ 80% (TEM).

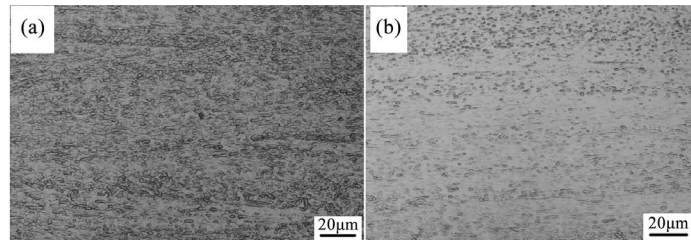


Figure 5. Microstructures of TC17 alloy deformed at: (a) 850°C 0.1 s⁻¹ 60%; (b) 850°C 10 s⁻¹ 60%.

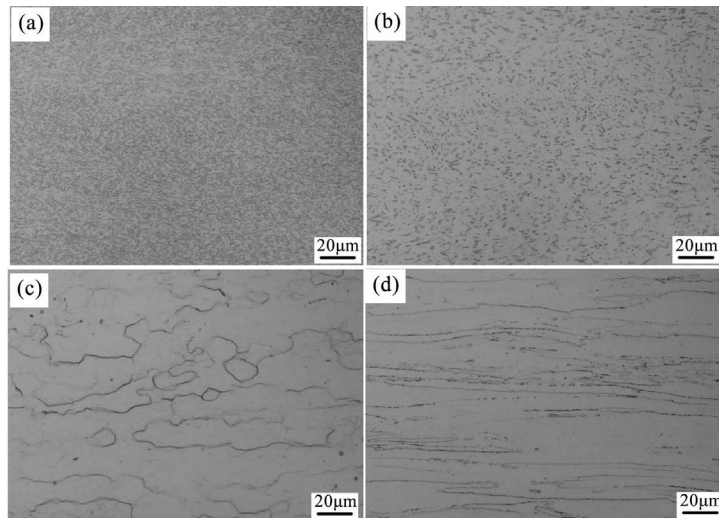


Figure 6. Microstructures of TC17 alloy deformed at: (a) 820°C 0.01s⁻¹ 60%; (b) 850°C 0.01 s⁻¹ 60%; (c) 930°C 0.01 s⁻¹ 60%; (d) 930°C 10 s⁻¹ 60%.

β region. The flow stresses were correlated with strain rate and the temperature by the constitutive equation. The conclusions can be summarized as follows:

1) All of the flow curves exhibit an initial peak at the beginning of deformation process. Then, the flow stress decreases sharply to a near steady state, which all curves exhibit flow softening behavior.

2) The deformation activation energy obtained in the $\alpha + \beta$ region for TC17 was 407 kJ/mol, and in the β region was 155 kJ/mol.

3) When it deforms in $\alpha + \beta$ two-phase region, increasing the deformation amount, reducing the strain rate or increasing the deformation temperature are beneficial to the α -phase spheroidization process; dynamic recrystallization occurring at the low strain rate in β single-phase region, dynamic response behavior is usually dominated by high strain rates.

Acknowledgements

The authors would like to acknowledge the financial support from Research Fund of Xi'an Aeronautical University, China (Grant No. 2018KY0102).

Conflicts of Interest

The authors declare no conflicts of interest regarding the publication of this paper.

References

- [1] Huang, B.Y., Li, C.G. and Shi, L.K. (2006) China Materials Engineering: Nonferrous Metal Materials Engineering (I). Vol. IV, Chemical Industry Press, Beijing.
- [2] Momeni, A. and Dehghani, K. (2010) Characterization of Hot Deformation Behavior of 410 Martensitic Stainless Steel Using Constitutive Equations and Processing Maps. *Materials Science & Engineering A: Structural Materials Properties Microstructure & Processing*, **527**, 5467-5473. <https://doi.org/10.1016/j.msea.2010.05.079>
- [3] Hradilová, M., Montheillet, F., Fraczkiewicz, A., *et al.* (2013) Effect of Ca-Addition on Dynamic Recrystallization of Mg-Zn Alloy during Hot Deformation. *Materials Science & Engineering A: Structural Materials Properties Microstructure & Processing*, **580**, 217-226. <https://doi.org/10.1016/j.msea.2013.05.054>
- [4] Berdjane, D., Fares, M.L. and Lemmoui, M.B.A.N. (2012) Deformation Behavior of a Nb-Ti-V Microalloyed Steel to Achieve, the HSLA X80 Grade by Simulation with a Torsion Test and Pilot Hot Rolling, Mill. *Revue de Métallurgie*, **109**, 465-475. <https://doi.org/10.1051/metal/2012042>
- [5] Werner, R., Schwaighofer, E., Schloffer, M., *et al.* (2014) Constitutive Analysis and Microstructure Evolution of the High-Temperature Deformation Behavior of an Advanced Intermetallic Multi-Phase γ -TiAl-Based Alloy. *Advanced Materials Research*, **922**, 807-812. <https://doi.org/10.4028/www.scientific.net/AMR.922.807>
- [6] Semiatin, S.L. and Jonas, J.J. (1984) Formability and Workability of Metals-Plastic Instability and Flow Localization. ASM, Metals Park, OH, 2419-2424.
- [7] Feng, L., Qu, H.L. and Zhao, Y.Q. (2004) High Temperature Deformation Behavior of TC21 Alloy. *Journal of Aeronautical Materials*, **24**, 11-13.
- [8] Wang, R.N., Qi, Z.P. and Zhao, Y.Q. (2008) High Temperature Plastic Deformation Behavior and Processing Diagram of Ti53311S Alloy. *Rare Metal Materials and Engineering*, **37**, 10-13.
- [9] Bai, X.F., Zhao, Y.Q., Zeng, W.D., *et al.* (2014) Effect of Deformation Parameters on Hot Deformation Behavior, Microstructure and Texture Evolution of TLM Titanium Alloy during Hot Compression. *Rare Metal Materials and Engineering*, **43**, 171-176.
- [10] Hong, Q., Han, D. and Guo, P. (2017) High Temperature Rheological Properties and Microstructure Evolution of TC4-DT Alloys. *Thermal Process Technology*, **7**, 181-182.
- [11] Luo, Y., Li, Y.Q. and Li, H. (2008) High Temperature Deformation Behavior and Flow Stress Model of TC4 Titanium Alloy. *Chinese Journal of Nonferrous Metals*, **18**, 1395-1401.
- [12] Zhao, Y.H., Ge, P. and Zhao, Y.Q. (2009) Study on Thermal Deformation Behavior of Ti-1300 Alloy. *Rare Metal Materials and Engineering*, **38**, 46-49.
- [13] Yu, Y.L., Pei, Z.P. and Zhao, Y.Q. (2008) Effect of Initial State on Thermal Deformation of Ti600 Titanium Alloy. *Rare Metal Materials and Engineering*, **37**, 622-624.
- [14] McQueen, H.J., Yue, S., Ryan, N.D. and Fry, E. (1995) Hot Working Characteristics of Steels in Austenitic State. *Journal of Materials Processing Technology*, **53**, 293-310. [https://doi.org/10.1016/0924-0136\(95\)01987-P](https://doi.org/10.1016/0924-0136(95)01987-P)
- [15] Shi, H., McLaren, J., Sellars, C.M., Shahani, R. and Bolingbroke, R. (1997) Constitutive Equations for High Temperature Flow Stress of Aluminum Alloys. *Materials Science and Technology*, **13**, 210-216. <https://doi.org/10.1179/mst.1997.13.3.210>